INSTITUT DE FRANCE
Académie des sciences

Comptes Rendus

Géoscience

Sciences de la Planète

Yves Moussallam, Clive Oppenheimer and Bruno Scaillet

A novel approach to volcano surveillance using gas geochemistry

Published online: 26 October 2022

https://doi.org/10.5802/crgeos.158

Part of Special Issue: Magma degassing and its impact on the Earth's atmosphere: from magma oceans to lava lakes

Guest editors: Manuel Moreira (Institut des Sciences de la Terre d'Orléans Université d'Orléans-CNRS-BRGM 1a rue de la Férollerie 45071 Orléans France), Bruno Scaillet (Institut des Sciences de la Terre d'Orléans Université d'Orléans-CNRS-BRGM 1a rue de la Férollerie 45071 Orléans France) and Clive Oppenheimer (Department of Geography, University of Cambridge, Downing Place, Cambridge CB2 3EN, UK)

Les Comptes Rendus. Géoscience — Sciences de la Planète *sont membres du Centre Mersenne pour l'édition scientifique ouverte*
www.centre-mersenne.org
e-ISSN : 1778-7025

Comptes Rendus
Géoscience — Sciences de la Planète
Published online: 26 October 2022
https://doi.org/10.5802/crgeos.158

Magma degassing and its impact on the Earth's atmosphere: from magma oceans to lava lakes / *Impact atmosphérique du dégazage magmatique : des océans de magma aux lacs de lave*

A novel approach to volcano surveillance using gas geochemistry

Yves Moussallam [a, b, *], **Clive Oppenheimer** [c] **and Bruno Scaillet** [d]

[a] Lamont-Doherty Earth Observatory, Columbia University, New York, USA

[b] Department of Earth and Planetary Sciences, American Museum of Natural History, New York, USA

[c] Department of Geography, University of Cambridge, Downing Place, Cambridge CB2 3EN, UK

[d] ISTO, 7327 Université d'Orléans-CNRS-BRGM, 1A rue de la Férollerie, 45071 Orléans cedex 2, France

E-mails: yves.moussallam@ldeo.columbia.edu (Y. Moussallam), co200@cam.ac.uk (C. Oppenheimer), bscaille@cnrs-orleans.fr (B. Scaillet)

Abstract. Identifying precursory phenomena is central to the short-range assessment and anticipation of volcanic hazards. The chemistry of gases, which may separate from magma at depth, is operationally monitored at many volcanoes worldwide to manage risk. However, owing to the complexity of volcanic degassing, decoding the message of gas geochemistry has proven challenging. Here, we report an approach to restoration of measured volcanic gas compositions that enables tracking of variations in the temperature and/or oxidation state of the source magma. We validate the approach with reference to independent estimates of melt oxidation state obtained by X-ray absorption near-edge structure (XANES) spectroscopy at the iron K-edge. We then apply the method to a global database of high temperature volcanic gases and to extended gas geochemical timeseries at Unzen, Aso, and Asama volcanoes, identifying hitherto unreported but significant changes in magma intensive parameters that preceded or accompanied changes in volcanic activity. Restoration of volcanic gas compositions offers a promising complement to monitoring strategies at active volcanoes, calling for more systematic operational surveillance of redox-sensitive gas species.

Keywords. Oxygen fugacity, Volcanic degassing, Volcanic gases, Redox, Volcano monitoring, Gas geochemistry.

Published online: 26 October 2022

1. Introduction

Volcanic gas measurements have been made for decades but their interpretation remains challenging. This challenge is particularly acute when gas observations and monitoring are applied to hazard assessment. The complexity arises from the multiple chemical and physical processes that can influence gas flux, atomic and molecular composition, and isotopic signature measured at the surface. These include processes occurring within stored or migrating magma (e.g., exsolution, gas separation which depends on pressure, temperature, melt composition, and magma permeability and ascent rate, etc.),

* Corresponding author.

within fracture networks in solid rock through which gases pass (e.g., gas–rock interaction, cooling and re-equilibration), and in mixing with other fluids (including hydrothermal fluids and air).

Increasingly systematic work on gas geochemistry began in the late 1950s to 1960s [Ellis, 1957, Matsuo, 1962]. In the 1980s and 1990s, several studies looked at the composition of volcanic gases collected at varying vent temperatures to identify process controlling their oxidation state. For instance, Giggenbach [1987] analysed fumarolic emissions (temperatures from 106 °C to 760 °C) at Whakaari/White Island (New Zealand). For high temperature gases, he identified three degassing scenarios: "A1", "A2" and "A3" [see Figure 16 in Giggenbach, 1987]. Scenario A1 involves direct rise of the gas phase to the surface without internal equilibration or equilibration with the vent system. In scenario A2, the gas maintains equilibrium with the magma throughout ascent, the oxidation state of the gas being buffered by and equal to that of the magma, while in A3, a "fluid-dominated" regime, gas oxidation state is largely controlled by internal equilibrium (though in Giggenbach 1987's description of the process, the gas could still exchange chemically with, and reduce, a stagnant melt).

Gerlach [1993] measured a series of high temperature volcanic gases with apparent equilibrium temperatures (AET) ranging from 935 °C to 1185 °C [see Ellis, 1957, Matsuo, 1962, Heald et al., 1963 for earliest definitions of AET], collected from fissures and lava flow skylights during the Pu'u 'Ō'ō eruption of Kīlauea. He found that the gas oxidation states (termed as, "apparent oxidation state" or AOS) plotted mostly parallel to rock redox buffers [see Figure 5 in Gerlach, 1993] and argued that redox equilibrium between the rock/magma and gas was maintained during cooling with buffering effective from molten to subsolidus conditions. This interpretation corresponds to scenario A2 of Giggenbach [1987] and is consistent with data and arguments of Allard et al. [1977] at Erta Ale, where they found the oxidation state of high temperature (1130 °C) volcanic gases to indicate equilibrium with the basaltic magma.

Shinohara et al. [1993] and Ohba et al. [1994] reported comparable studies of high temperature gases emitted from Satsuma-Iwojima and Unzen volcanoes, respectively. They concluded that addition of external water might play a role but found that temperature-oxygen fugacity (T–fO_2) relationships could be explained by the equilibrium:

$$SO_2 + 3H_2 = H_2S + 2H_2O \quad (1)$$

This corresponds to an internal re-equilibration of the gas phase, essentially Giggenbach's scenario A3. Internal re-equilibration appears (though they do not make this explicit) also to be the process favoured by Menyailov et al. [1986], who measured 740 °C to 895 °C emissions from Momotombo between 1974 and 1984. They found the oxidation state of hotter gases to be closer to the quartz-fayalite-magnetite (QFM) buffer while that for cooler gases to be closer to the nickel–nickel oxide (NNO) buffer.

In the following decades, the view that the oxidation state of volcanic gases is buffered by the magma/rock during ascent and cooling (scenario A2) became generally accepted, exemplified by the wide-ranging synthesis of Symonds et al. [1994], who concluded that "lavas buffer fO_2 in high temperature volcanic gases".

More recently, Oppenheimer et al. [2018] argued that large variation in gas composition during degassing at the Kilauea lava lake over a 850 °C to 1110 °C range in AET could be explained by closed system, gas-only cooling and re-equilibration [see Figure 3 in Oppenheimer et al., 2018]. Compiling a global database of high temperature ($T \geq 600$ °C) volcanic gases, Moussallam et al. [2019b] explained the T–fO_2 trend of the entire database by closed system, gas-only cooling and internal re-equilibration according to equilibrium (1) [see Figure 4A in Moussallam et al., 2019b]. Both studies argue for the role of scenario A3 in explaining volcanic gas chemistry and confirm that emissions quench with negligible oxidation in air [e.g., Aiuppa et al., 2007, Martin et al., 2009], such that they preserve a signature of the original magmatic gas modified only by internal re-equilibration during cooling.

Here, we develop the application of these findings for interpretation of redox-sensitive species measured in high-temperature volcanic emissions. Taking the assumption that emitted gases cool from magmatic temperature following separation from their source melts, we explore estimation of either T or fO_2 when finally in equilibrium with the magma. As the system is underdetermined, a further assumption of either the degree of gas cooling, or the magma oxidation state, is however necessary. We test the approach by comparing our results with indepen-

dent determinations of melt oxidation state, before applying it to analysis of multiyear datasets of gas emissions from Uzen, Aso and Asama volcanoes and to a global database of volcanic gas observations.

2. Methodology

We used the global dataset of high temperature volcanic gases compiled by Moussallam et al. [2019b], supplemented with recently available data (Table S1). The dataset is limited to high temperature (>500 °C) gases, for which gas–rock or gas–fluid interactions are minimal [e.g., Giggenbach, 1996, Symonds et al., 2001]. To quantify the cooling of volcanic gases between their escape from the melt and their last retained equilibrium temperature, we extended the compilation of Moussallam et al. [2019b], collecting melt temperature estimates from existing literature, mostly from petrological studies (i.e., geothermometry). In cases where such data were unavailable (the case for ten of the 37 volcanoes), we estimated melt temperature from reported bulk composition. The difference between estimated melt temperature and measured (or calculated) gas emission (or apparent equilibrium) temperature yields the amount of closed system cooling experienced by the gas. Using the reported gas composition as starting conditions, we restored each to its values at melt temperature by solving equilibrium (1) at 1 bar using thermodynamic parameters given in Ohba et al. [1994] for the temperature-dependent equilibrium constant (K) and recalculating the gas composition such that $K(T) = \log(X_{SO_2}^{-1} X_{H_2}^{-3} X_{H_2S} X_{H_2O}^{2}) - \log(P)$, where X_i represents the mole fraction of component i, subject to the constraints, that the amounts of O, H and S in the gas mixture remain constant.

2.1. *Example of restoration calculation*

In this section, we elaborate the calculation method used in this study through a worked example. We take the case of volcanic gases measured in 1994 from the then active lava dome of Merapi volcano (Indonesia), in the course of the fifth International Association of Volcanology and Chemistry gas workshop [Giggenbach et al., 2001]. Gases were collected directly at the vent (Gendol fumarole) and had an exit temperature of 803 °C. Proportions (median of six analyses) of H_2O, CO_2, SO_2, CO, H_2S and H_2 gases were found to be 88.7, 5.56, 0.98, 0.0235, 0.13 and 0.5 mol%, respectively [Giggenbach et al., 2001]. This gas analysis was employed also by Moussallam et al. [2019b, see methodology section] to illustrate the calculation of the AET and AOS. We pick up from this point to demonstrate restoration of either (i) the oxidation state at equilibrium with the magma if the magmatic temperature is known or (ii) the temperature at equilibrium with the magma if the magma oxidation state is known.

Costa et al. [2013] estimated temperatures for the Merapi magma of 900 to 1000 °C based on amphibole thermobarometry in products of the 2006 and 2010 eruptions. We use the median temperature of 950 °C as the magmatic temperature (T_{mag}) in this example. The AET of the Merapi gas mixture measured by Giggenbach et al. [2001] can be calculated by the H_2/H_2O and H_2S/SO_2 method, yielding an AET of 849 °C, or by the H_2S/SO_2 and CO/CO_2 method, yielding an AET of 790 °C [see Moussallam et al., 2019b for step-by-step calculation]. Since in this example the exit temperature (803 °C) was measured directly by thermocouple by Giggenbach et al. [2001] we use this value as the starting equilibrium temperature of the gas mixture. To calculate the AOS, we can use either the H_2S/SO_2 and T method, yielding an AOS of $\log fO_2$ of −13.75 or the H_2/H_2O and T method yielding an AOS of $\log fO_2$ of −14.02 [see Moussallam et al., 2019b, for step-by-step calculation]. We use the second estimate in this example, which corresponds to QFM + 0.6. Now that the starting (AET and AOS) and final (T_{mag}) conditions are defined, we can proceed with the calculation.

The equilibrium constant (K) of reaction (1) ($SO_2 + 3H_2 = H_2S + 2H_2O$) can be written (assuming all fugacity coefficients are (1) as $\log K_1(T) = \log(X_{SO_2}^{-1} X_{H_2}^{-3} X_{H_2S} X_{H_2O}^{2}) - \log(P)$, where X_i represents the mole fraction of component i. The equilibrium constant can also be written as $\log K_2 = A + BT^{-2} + CT^{-1} + DT + E \ln T$, where A, B, C, D, and E are constants with values of 8.5667, −29,743, 10,449, 0.00047814 and −1.7784, respectively [taken from Ohba et al., 1994 who obtained them from thermodynamic data at 1 bar in the NIST database of Chase, 1998]. K_2 can be calculated at any temperature. The problem is then to find X_{SO_2},

X_{H_2}, X_{H_2S}, and X_{H_2O}, at any temperature of interest such that $K_1 = K_2$. Because there are four unknowns, the solution isn't unique. However, we can assume the gas composition in terms of atomic (O, H and S) species as constant. We can then use a solver to find the values of X_{SO_2}, X_{H_2}, X_{H_2S}, and X_{H_2O} that satisfies all the constraints and then from those, calculate an AOS at the temperature of interest. For the Merapi 1994 case, the initial X_{SO_2}, X_{H_2}, X_{H_2S}, and X_{H_2O} values are 0.0102, 0.0052, 0.0013 and 0.9191, respectively, at an AET of 803 °C (AOS of $\log fO_2 = -14.02 = \text{QFM} + 0.6$). At a T_{mag} of 950 °C, a solution to $K_1 = K_2$ at fixed O, H and S species gives values of 0.0104, 0.0094, 0.0011 and 0.9151 for X_{SO_2}, X_{H_2}, X_{H_2S}, and X_{H_2O}, respectively. This solution corresponds to an AOS at magmatic temperature of $\log fO_2 = -11.81 = \text{QFM} + 0.1$.

The same procedure can be applied in the case where T_{mag} is unknown but the gas oxidation state at equilibrium with the melt (i.e., the melt oxidation state) is known. The calculations are performed starting at the initial AET and by increasing T incrementally until the AOS matches the target value. This value represents the temperature at equilibrium with the magma.

All results presented in this study were performed at a fixed pressure of 1 bar. While this is a simplification, we note that these types of calculations reproduce the variability found in natural observations extremely well, both in global compilations [Moussallam et al., 2019b] and for individual volcanoes [Oppenheimer et al., 2018]. We stress that the application of the method is limited to high temperature (>500 °C) magmatic gases for which gas–rock or gas–fluid interactions are minimal [e.g., Giggenbach, 1996, Symonds et al., 2001].

3. Results

Initial conditions and final calculations are reported in Table S2. Figure 1 shows the oxidation state of volcanic gases from our global database plotted against the estimated closed system cooling they have experienced. The dataset shows a clear global trend towards oxidation of the gases as a function of cooling, as reported by Moussallam et al. [2019b]. Figure 1 shows the restorations of the oxidation state of each volcanic gas along individual cooling paths, back to magmatic temperatures. While original gas oxidation states vary by five log units (from $\log fO_2 = \text{QFM} + 4.1$ to $\text{QFM} - 0.9$), restored oxidation states at magmatic temperature vary within two log units (from $\log fO_2 = \text{QFM} + 0.7$ to $\text{QFM} - 1.1$). Arc magmas are represented with a near normal distribution with an average of $\log fO_2 = \text{QFM} + 0.0$ and standard deviation of ±0.3 (the median is also QFM). This is somewhat more reduced than suggested by petrological estimates, being closer to inferred arc mantle conditions (see compilation in Matjuschkin et al. [2016] and their Figure 1), possibly reflecting changes in oxidation state on decompression [e.g., Burgisser and Scaillet, 2007]. Intraplate magmas are poorly represented in our database but tend to be more reduced, with an average of $\text{QFM} - 0.5$ log units.

4. Discussion

4.1. *Method validation*

To test the validity of the approach and the underlying assumptions, we compare the restored oxidation state of volcanic gases at magmatic temperature to independent determinations of melt oxidation state by X-ray absorption near-edge structure (XANES) spectroscopy at the iron K-edge. Iron K-edge XANES in silicate glasses is a synchrotron-based technique used for the determination of the relative proportions of ferric (Fe^{3+}) and ferrous (Fe^{2+}) iron. The small (typically 2 to 10 μm) beam size achievable allows measurements of melt inclusions and matrix glasses that can be converted to oxygen fugacity (fO_2) using the equation provided by Kress and Carmichael [1991] [full method detailed in Rose-Koga et al., 2021]. Since melt oxidation state varies with differentiation [e.g., Kelley and Cottrell, 2012] and degassing [e.g., Moussallam et al., 2014, 2016, 2019a], measurements must pertain to the time period when gas observations were made. We identified suitable measurements for four volcanoes: (i) Erta Ale, where gas measurements were made in January 2011 [Zelenski et al., 2013], and November 2010 scoriae were analysed by XANES [de Moor et al., 2013]. (ii) Etna, where gas measurements from 2009 at the Voragine and Bocca Nuova craters [Aiuppa et al., 2011] are compatible with 2002–2013 tephra investigated by XANES [Gennaro et al., 2020]. (iii) Kīlauea, where gas measurements in 2013 [Oppenheimer et al., 2018] are comparable in timing with

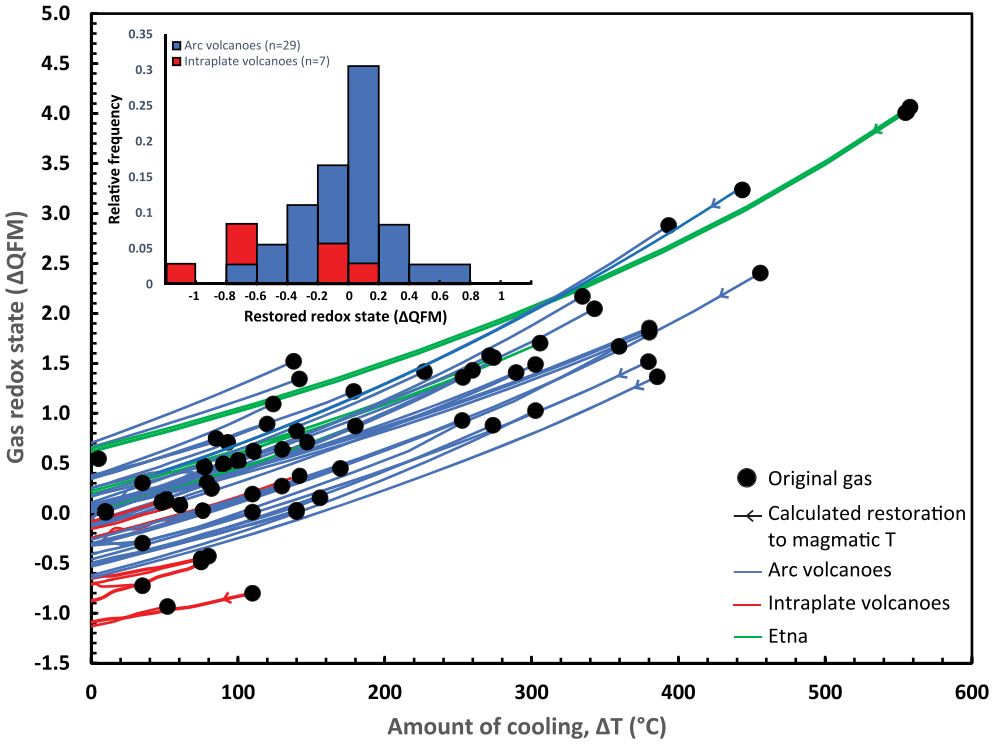

Figure 1. Oxidation state of volcanic gases (expressed as deviation from the QFM buffer) as a function of the difference between AET and the temperature of the associated melt. Lines show the results of recalculating the oxidation state of each gas composition back to its magmatic temperature. Upper left inset: non-stacked histogram showing the frequency of oxidation states (expressed as deviation from the QFM buffer) of arc and intraplate melts calculated by restoring volcanic gas compositions to their magmatic temperature.

2008 and 2010 tephra measured by XANES [Moussallam et al., 2016]. (iv) Surtsey, where gases collected in 1965 [Sigvaldason and Elísson, 1968] [summarised in Gerlach, 1980] can be compared with XANES measurements of tephra erupted between 1963 and 1966 [Schipper and Moussallam, 2017].

The results are shown in Figure 2. Three of the four volcanoes investigated lie within one standard deviation of the 1:1 line. Gas and melt oxidation state data from Surtsey, however, differ by 0.4 $\log fO_2$ units. In this case, the gas data were collected at 1125 °C, close to the estimated magmatic temperature of 1160 °C, so our calculations only slightly shifted the AOS. The broad agreement between restored oxidation state of volcanic gases at magmatic temperature and independently constrained melt oxidation state provides a first order corroboration of our approach. We note that there is no correlation between the oxidation state of restored volcanic gases and melt temperature (Figure S1).

4.2. *Monitoring magma oxidation state and/or temperature at active volcanoes*

To explore the application of the method, we apply it to three sets of observations from different volcanoes in Japan. In each case, the four species in equilibrium (1) were monitored in high-temperature gas emissions for extended periods. The first case pertains to two fumaroles, 20 m apart, on an active lava dome at Mt Unzen [Ohba et al., 2008], and for which the gas observations can be evaluated in the context of detailed petrological information. The gases, whose exit temperatures differed, were sampled six times between May 1992 and October 1993. Unzen erupted 900 °C dacitic magmas generated from mixing of

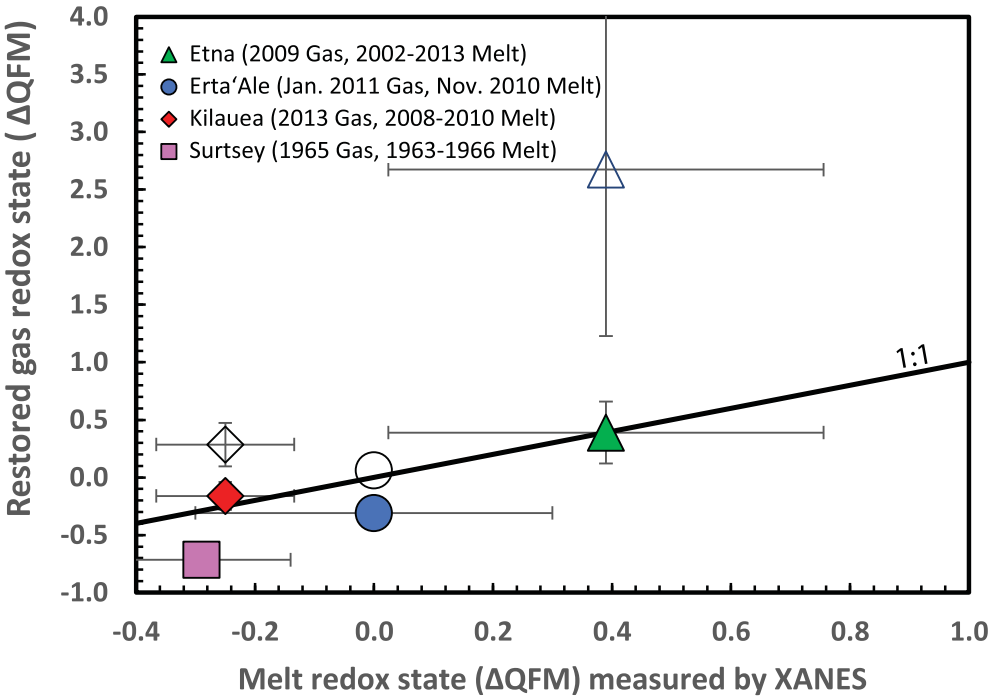

Figure 2. Restored oxidation state of volcanic gases (expressed as deviation from the QFM buffer) at magmatic temperature compared to oxidation state of corresponding melts measured by XANES on melt inclusions and matrix glasses. Gas measurements from Etna, Erta Ale, Kīlauea and Surtsey are from Aiuppa et al. [2011], Zelenski et al. [2013], Oppenheimer et al. [2018], and Sigvaldason and Elísson [1968] [as reported in Gerlach, 1980] respectively. XANES measurements are from de Moor et al. [2013], Gennaro et al. [2020], Moussallam et al. [2016], and Schipper and Moussallam [2017] respectively. Symbols are average values, error bars represent one standard deviation on the set of measurements used to calculate each average. Unfilled symbols show gas AOS prior to restoration.

andesite (1030 °C) and rhyodacite (800 °C) endmembers [Venezky and Rutherford, 1999]. While the AOS and AET of the gases varied widely (from QFM + 0.2 to QFM + 3.2 log units, and from 469 to 878 °C, respectively), once restored to a magmatic temperature of 900 °C, all measurements converge at $\log fO_2$ = QFM + 0.03 with a standard deviation of ±0.04 (Figure 3A).

If we restore the gas measurements to a fixed fO_2 ($\log fO_2$ = QFM + 0.03), then we can calculate temperature variations. These suggest an increase in T_{mag} of around 30 °C from May 1992 to February 1993, consistent with a decrease of around 0.7 wt% SiO_2 in the erupted dacite (implying augmentation of the andesitic component) [Nakada and Motomura, 1999]. A subsequent decrease in calculated melt temperature in October 1993 mirrors a trend of increasing silicate content (Figure 3B). This interpretation is compatible with FeTi-oxide evidence, which suggests a groundmass temperature variation of 100 °C spanning the 1991–95 eruption and an overall 2 wt% variation in bulk SiO_2 content [Nakada and Motomura, 1999]. In the Unzen case, temporal variations in the restored syn-eruptive gases are minor, mirroring equally limited changes in the erupted magma. In the following case studies, restored gases record much larger variations.

The second case is that of Aso volcano spanning from 2003 until an eruption on 25 November 2014. We restored the data for gas emissions from Nakade crater [Shinohara et al., 2018] back to a magmatic temperature of 1067 °C, the median value estimated for erupted lava in 2014 [Saito et al., 2018; Figure 4A]. Assuming constant temperature, the computed melt oxidation state changed significantly in early 2012 to 2013 (Figure 5A). Until early 2012, the

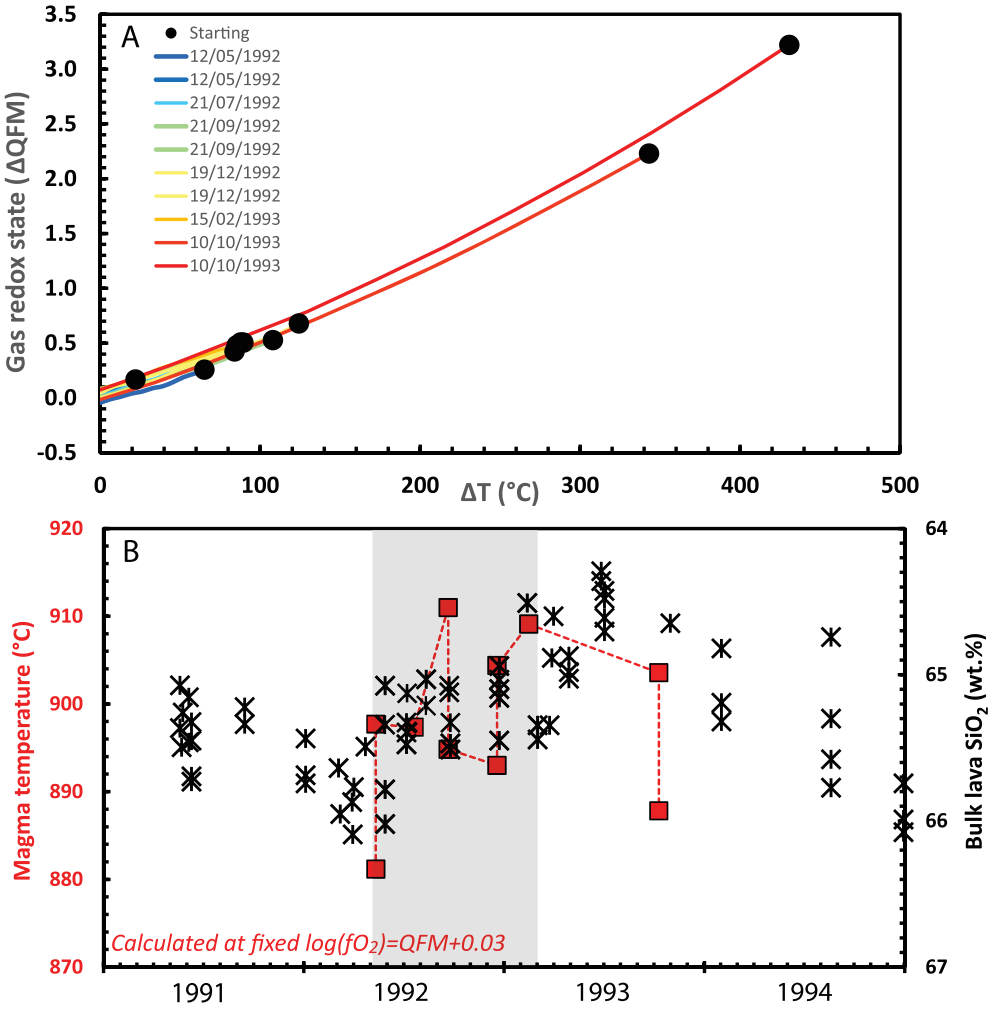

Figure 3. (A) Oxidation state of volcanic gases emitted at Unzen volcano (expressed as deviation from the QFM buffer) as a function of the difference between AET (apparent equilibrium temperature) and melt temperature. Lines show the results of recalculating the oxidation state of each gas composition back to its magmatic temperature. Starting conditions take gas compositions from direct sampling of two fumaroles from the active lava dome at Unzen between 1992 and 1993 [Ohba et al., 2008]. (B) Evolution of the melt temperature at Unzen calculated from restored gas composition assuming a fixed melt oxidation state of $\log fO_2 = \mathrm{QFM} + 0.03$ compared with bulk rock composition (in SiO_2 content) of the extruded dacitic dome lava [black crosses, from Nakada and Motomura, 1999]. Light grey shaded regions correspond to the period from May 1992 to February 1993 discussed in text.

calculated melt oxidation state varies from QFM + 0.1 to QFM − 0.3 log units (average of QFM − 0.1 and standard deviation of 0.1). From 2012 to 2014, the calculated melt oxidation state varies from QFM − 0.3 to QFM − 0.6 log units (average of QFM − 0.4 and standard deviation of 0.05). Alternatively, if we fix the melt oxidation state (e.g., at QFM), we can compute melt temperature (Figure 5B). Under this assumption, prior to 2012, the calculated melt temperature varies from 991 to 1094 °C (average of 1041 ± 32 °C), while between 2012 and 2014, it varies from 948 to 980 °C (average of 963 ± 11 °C).

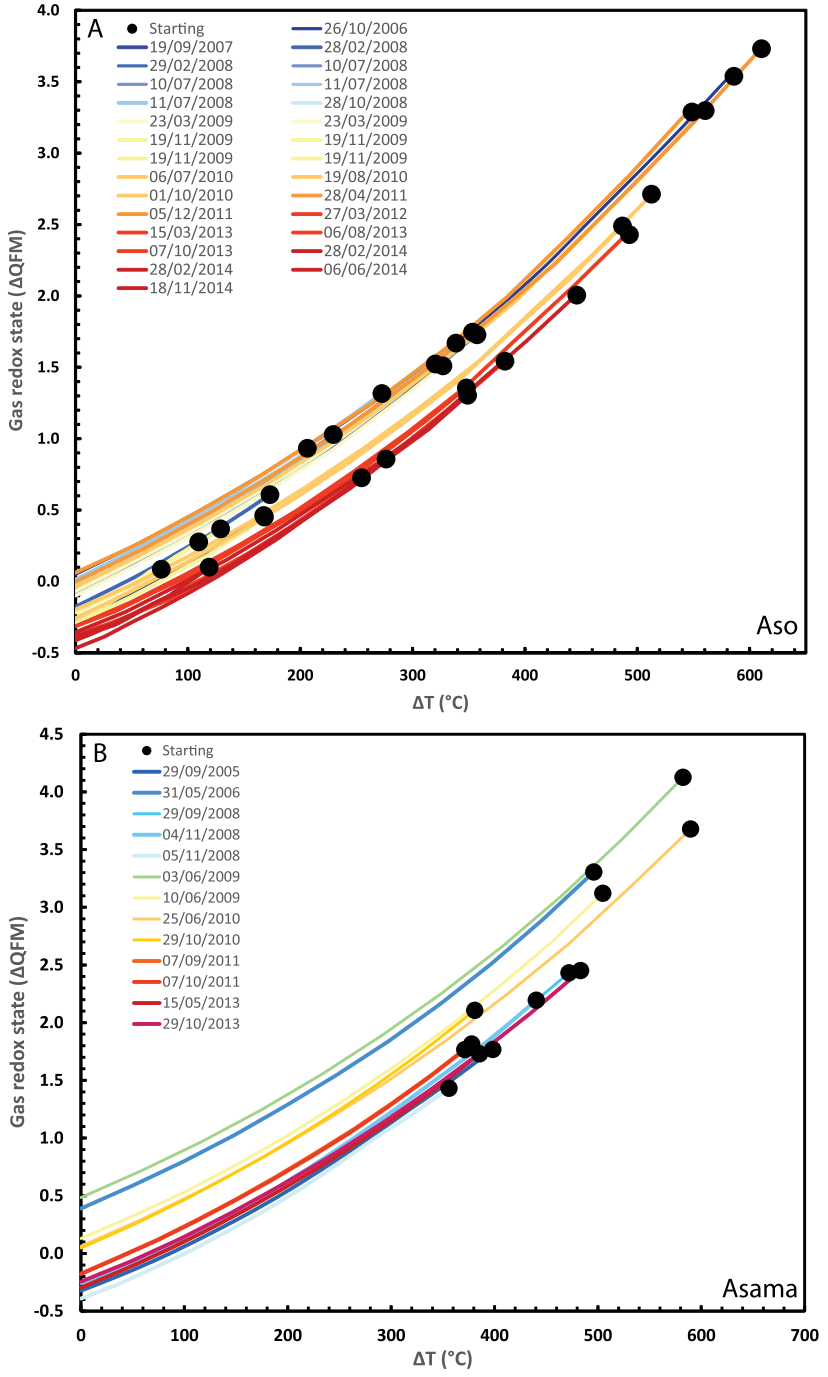

Figure 4. Oxidation state of volcanic gases emitted by Aso (A) and Asama (B) volcanoes (expressed as deviation from the QFM buffer) as a function of the difference between AET (apparent equilibrium temperature) and melt temperature. Lines show the results of recalculating the oxidation state of each gas composition back to its magmatic temperature, solving for the reaction $SO_2 + 3H_2 = H_2S + 2H_2O$ at 1 bar using thermodynamic parameters in Ohba et al. [1994]. Starting conditions for Aso take gas compositions reported by Shinohara et al. [2018] for fumaroles gases measured by MultiGAS prior to the 25 November 2014 eruption. Starting conditions for Asama use gas compositions reported by Shinohara et al. [2015].

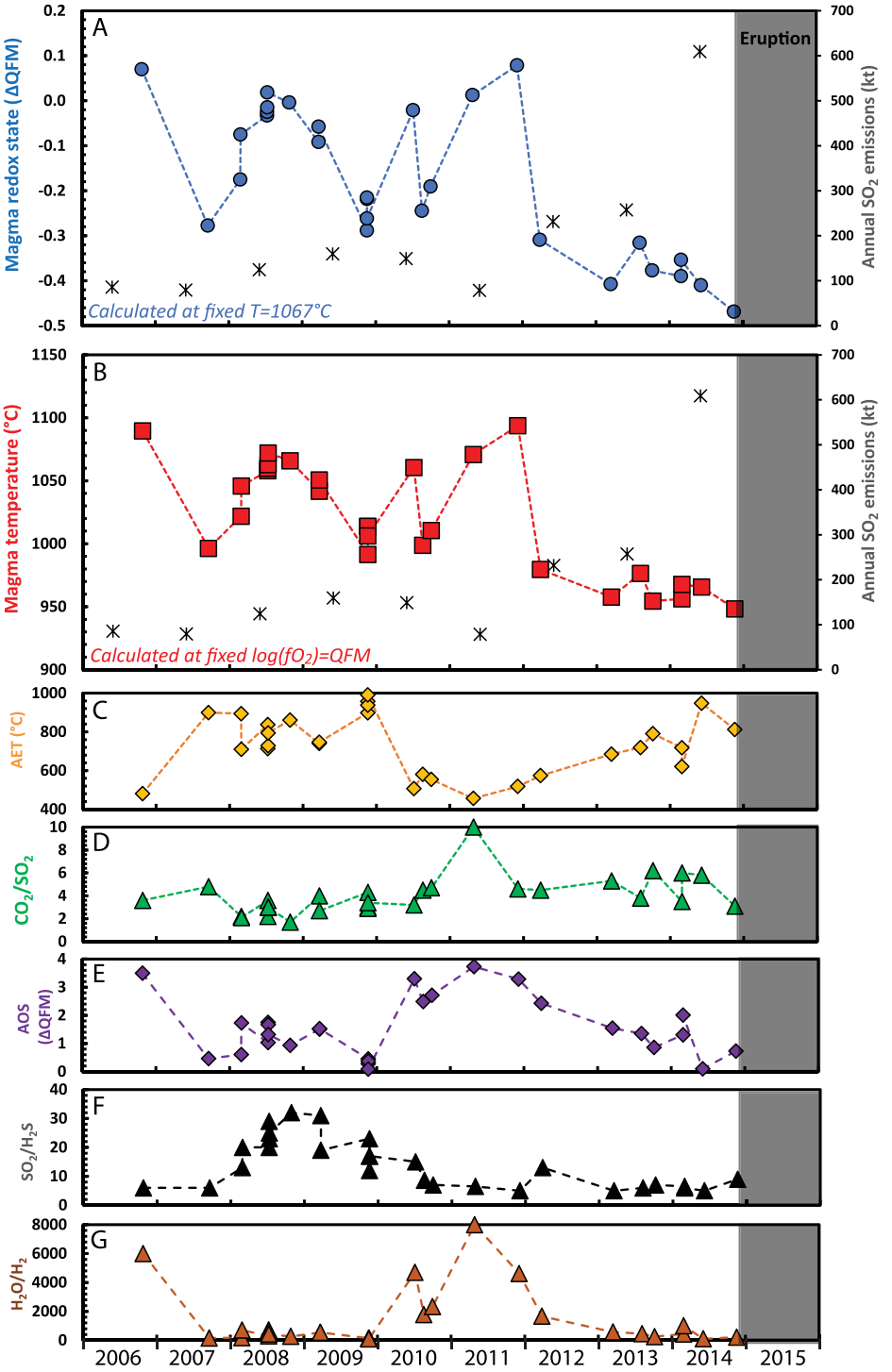

Figure 5. Evolution of the melt conditions at Aso volcano calculated from restored gas composition assuming (A) a fixed melt temperature of 1067 °C and (B) a fixed melt oxidation state of log fO_2 = QFM+0.0. SO_2 emission rate measurements in A and B (black crosses) are calendar-year averages OMI data from Carn et al. [2017] plotted mid-year. (C–G) Evolution of the apparent equilibrium temperature (AET), CO_2/SO_2 ratio, apparent oxidation state (AOS), SO_2/H_2S and H_2O/H_2 ratios from the original gas measurements [Shinohara et al., 2018].

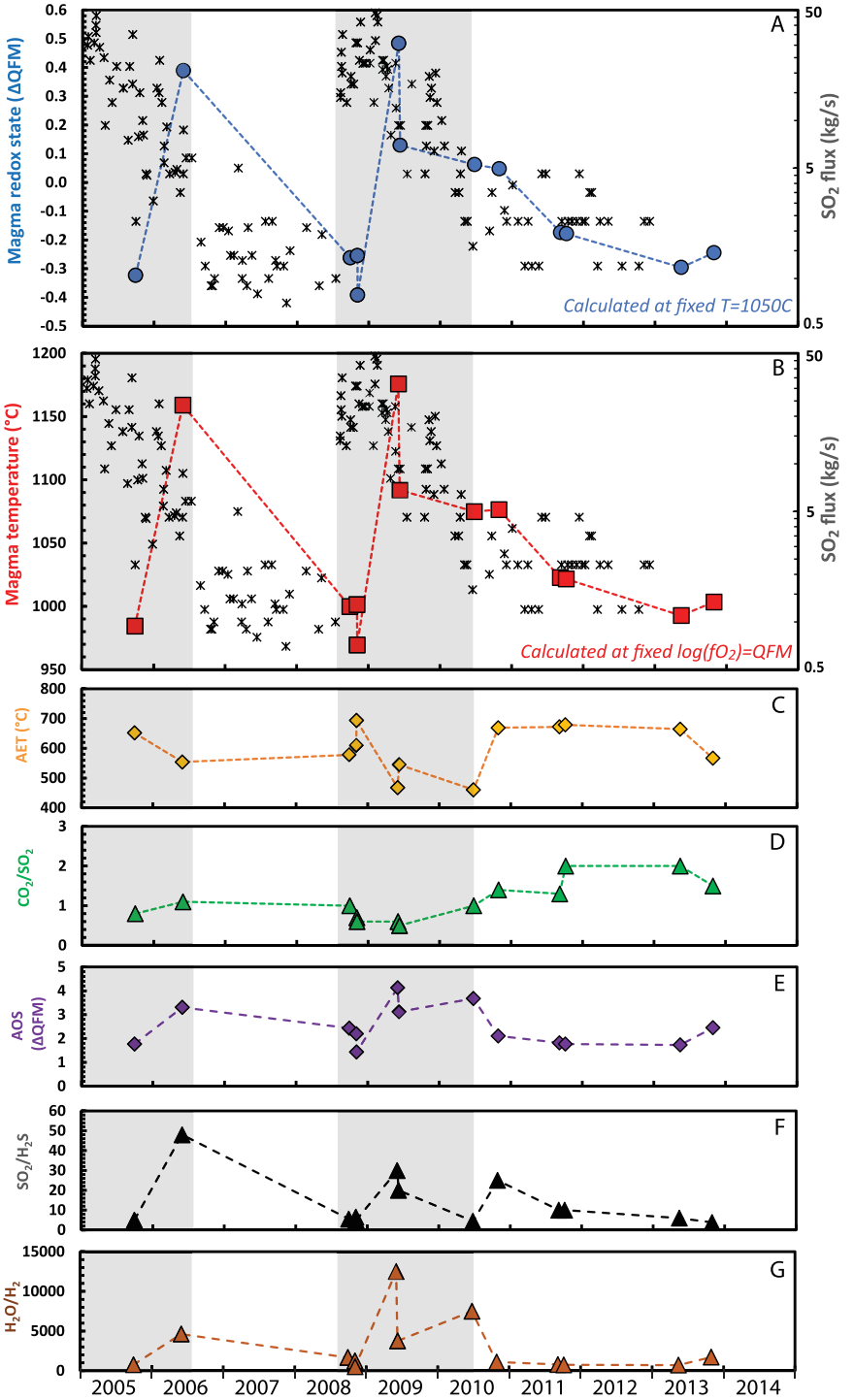

Figure 6. Caption continued on next page.

Figure 6. (**cont**.) Evolution of the melt conditions at Asama volcano calculated from restored gas composition assuming (A) a fixed melt temperature of 1050 °C and (B) a fixed melt oxidation state of $\log fO_2$ = QFM + 0.0. SO_2 flux measurements in (A) and (B) (black crosses) are from Ohwada et al. [2013] (C–G). Evolution of the apparent equilibrium temperature (AET) and CO_2/SO_2 ratio, apparent oxidation state (AOS), SO_2/H_2S and H_2O/H_2 ratios from the original gas measurements [Shinohara et al., 2015]. Light grey shaded regions correspond to periods of stronger degassing [Ohwada et al., 2013, Shinohara et al., 2015].

The apparent change in intensive conditions of the magma in 2012–2013 that we reveal might, with hindsight, be viewed an eruption precursor. It precedes a falling lake level in late 2013 [Shinohara et al., 2018], and the opening of a new vent in January 2014 [Ichimura et al., 2018], which was accompanied by a three-fold increase in SO_2 emission rates (Figure 5A and B) and an abrupt increase in seismicity in late August 2014 [Sandanbata et al., 2015]. We note that the unrestored data for 2012–2014 show no systematic excursions from baseline levels spanning the period 2006 to 2011, neither in major gas ratios such as CO_2/SO_2, H_2O/H_2, SO_2/H_2S nor in AET or AOS (Figure 5C–G).

The cooling inferred by calculations at fixed redox state could signify ascent and cooling of magma at shallow levels. Conversely, a reduction in melt oxidation state prior to eruption (for the fixed temperature calculations) could indicate reduction due to sulphur degassing on magma ascent [e.g., Anderson and Wright, 1972, Métrich et al., 2009, Moussallam et al., 2014, 2016, 2019a]. A combination of cooling and reduction is likely but cannot be disambiguated with the available gas data. We stress, however, that the gas restoration provides a unique locus for T–fO_2, in which temporal trends are evident (Figure 4). Petrological study of products of the 2014 eruption [Saito et al., 2018; using the melt, olivine–liquid, plagioclase–liquid and clinopyroxene–liquid geothermometers of Putirka, 2008] indicate a melt temperature of 1042–1092 °C, with melt inclusion compositions comparable to that of the groundmass and recording estimated temperatures of 1027–1081 °C.

Our third case pertains to Asama volcano spanning from 2004 to 2014, during which there were two periods of strong degassing and increased seismicity accompanying minor eruptions [Shinohara et al., 2015]. Asama gases were restored back to a magmatic temperature of 1050 °C, based on estimates made for eruptions in 2004 [Shimano et al., 2005]. This implies significant variation in melt oxidation state between QFM − 0.4 and QFM + 0.5 log units over the observation period (Figure 6A). Alternatively, fixing the melt oxidation state (at QFM) suggests substantial melt temperature variation between 955 and 1240 °C (Figure 6B). The trends in changing magmatic conditions show some correspondence with variations in gas emission rates (Figure 6A,B), with the two spikes in melt temperature and/or oxidized conditions coinciding with the two periods of stronger gas emission and minor explosions (whose ejecta, at least in 2009, include only traces of juvenile material [Maeno et al., 2010]).

Closer inspection suggests the elevated SO_2 emissions preceded changes in magmatic conditions whose relative variations more closely mirror trends in seismicity [see Figure 3b in Ohwada et al., 2013]. In contrast, the unrestored gas data show no systematic variations during, or prior to the periods of enhanced activity, neither in major gas ratios such as CO_2/SO_2, H_2O/H_2, SO_2/H_2S nor in AET or AOS (Figure 6C–G). Again, it is impossible to disambiguate changes in magma temperature from changes in oxidation state with the available data but the large variations evident in the end-member scenarios suggest a combination of the two processes since temperatures of 1240 °C are excessive, as are variations of melt oxidation state of nearly one log unit in fO_2 within a year. The spikes in both parameters may indicate episodic supply of hotter and more oxidised magma to a relatively small magma chamber unable to buffer the changes rapidly.

5. Conclusion

We have restored the composition of high temperature volcanic gases, drawing from published data, back to their magmatic temperature. We found that our restored gas oxidation states at magmatic

temperature are consistent with the oxidation state of corresponding melts, where measured independently. We applied the restoration procedure to a global database of volcanic gases and found that the wide variation in oxygen fugacity indicated in the original dataset is greatly lessened when gases are restored to magmatic temperature. The oxidation state of arc magmas that we calculate from restored gas measurements shows a normal distribution centred on $\log fO_2 = \mathrm{QFM} + 0.0 \pm 0.3$.

Our gas restoration approach further opens up the potential for applying gas monitoring data to track changes in magma oxidation states in real time if magma temperature is known, or to track changes in magma temperatures if magma oxidation state is known. Our reassessments of Unzen, Aso and Asama datasets suggest the potential to monitor, and sometimes discriminate between (given independent constraints) these parameters. We suggest that the operational application of the approach can complement monitoring and hazard assessment, revealing variations not evident from raw geochemical data and which may relate to critical processes known to drive abrupt changes in surface activity (including magma ascent and magma mixing). This requires careful attention to measurements of redox-sensitive gas species, which can be achieved using combinations of electrochemical sensors and spectrometric techniques.

Conflicts of interest

Authors have no conflict of interest to declare.

Acknowledgements

CO receives support from NERC (UKRI) under Highlight Topic "V-PLUS". BS acknowledges support from both LabEx VOLTAIRE (LABX-100-01) and EquipEx PLANEX (ANR-11-EQPX-0036) projects. We are grateful to Giovanni Chiodini for his review of an earlier version of this manuscript and to an anonymous reviewer.

Supplementary data

Supporting information for this article is available on the journal's website under https://doi.org/10.5802/crgeos.158 or from the author.

References

Aiuppa, A., Franco, A., Glasow, R. V., Allen, A. G., D'Alessandro, W., and Mather, T. A. (2007). The tropospheric processing of acidic gases and hydrogen sulphide in volcanic gas plumes as inferred from field and model investigations. *Atmospheric Chem. Phys.*, 7, 1441–1450.

Aiuppa, A., Shinohara, H., Tamburello, G., Giudice, G., Liuzzo, M., and Moretti, R. (2011). Hydrogen in the gas plume of an open-vent volcano, Mount Etna, Italy. *J. Geophys. Res.*, 116, article no. B10204.

Allard, P., Le Guern, F., and Sabroux, J. C. (1977). Thermodynamic and isotopic studies in eruptive gases. *Geothermics*, 5, 37–40.

Anderson, A. T. and Wright, R. (1972). Phenocrysts and glass inclusions and their bearing on oxidation and mixing of basaltic magmas, Kilauea Volcano, Hawaii. *Am. Mineral.*, 57, 188–216.

Burgisser, A. and Scaillet, B. (2007). Redox evolution of a degassing magma rising to the surface. *Nature*, 445, 194–197.

Carn, S. A., Fioletov, V. E., McLinden, C. A., Li, C., and Krotkov, N. A. (2017). A decade of global volcanic SO_2 emissions measured from space. *Sci. Rep.*, 7, article no. 44095.

Chase, M. W. (1998). *NIST-JANAF Thermochemical Tables*. American Chemical Society; American Institute of Physics for the National Institute of Standards and Technology, Washington, DC; Woodbury, NY.

Costa, F., Andreastuti, S., Bouvet de Maisonneuve, C., and Pallister, J. S. (2013). Petrological insights into the storage conditions, and magmatic processes that yielded the centennial 2010 Merapi explosive eruption. *J. Volcanol. Geotherm. Res.*, 261, 209–235. Merapi eruption.

de Moor, J. M., Fischer, T. P., Sharp, Z. D., King, P. L., Wilke, M., Botcharnikov, R. E., Cottrell, E., Zelenski, M., Marty, B., Klimm, K., Rivard, C., Ayalew, D., Ramirez, C., and Kelley, K. A. (2013). Sulfur degassing at Erta Ale (Ethiopia) and Masaya (Nicaragua) volcanoes: Implications for degassing processes and oxygen fugacities of basaltic systems. *Geochem. Geophys. Geosyst.*, 14, 4076–4108.

Ellis, A. J. (1957). Chemical equilibrium in magmatic gases. *Am. J. Sci.*, 255, 416–431.

Gennaro, E., Paonita, A., Iacono-Marziano, G., Moussallam, Y., Pichavant, M., Peters, N., and Martel, C.

(2020). Sulphur behaviour and redox conditions in Etnean magmas during magma differentiation and degassing. *J. Petrol.*, 61, article no. egaa095.

Gerlach, T. M. (1980). Evaluation of volcanic gas analysis from surtsey volcano, iceland 1964–1967. *J. Volcanol. Geotherm. Res.*, 8, 191–198.

Gerlach, T. M. (1993). Oxygen buffering of Kilauea volcanic gases and the oxygen fugacity of Kilauea basalt. *Geochim. Cosmochim. Acta*, 57, 795–814.

Giggenbach, W. F. (1987). Redox processes governing the chemistry of fumarolic gas discharges from White Island, New Zealand. *Appl. Geochem.*, 2, 143–161.

Giggenbach, W. F. (1996). Chemical composition of volcanic gases. In Scarpa, R. and Tilling, R. I., editors, *Monitoring and Mitigation of Volcano Hazards*, pages 202–226. Springer, Berlin, Heidelberg.

Giggenbach, W. F., Tedesco, D., Sulistiyo, Y., Caprai, A., Cioni, R., Favara, R., Fischer, T. P., Hirabayashi, J.-I., Korzhinsky, M., Martini, M., Menyailov, I., and Shinohara, H. (2001). Evaluation of results from the fourth and fifth IAVCEI field workshops on volcanic gases, Vulcano island, Italy and Java, Indonesia. *J. Volcanol. Geotherm. Res.*, 108, 157–172.

Heald, E. F., Naughton, J. J., and Barnes, I. L. (1963). The chemistry of volcanic gases: 2. Use of equilibrium calculations in the interpretation of volcanic gas samples. *J. Geophys. Res.*, 68, 545–557.

Ichimura, M., Yokoo, A., Kagiyama, T., Yoshikawa, S., and Inoue, H. (2018). Temporal variation in source location of continuous tremors before ash–gas emissions in January 2014 at Aso volcano, Japan. *Earth Planets Space*, 70, article no. 125.

Kelley, K. A. and Cottrell, E. (2012). The influence of magmatic differentiation on the oxidation state of Fe in a basaltic arc magma. *Earth Planet. Sci. Lett.*, 329–330, 109–121.

Kress, V. C. and Carmichael, I. S. E. (1991). The compressibility of silicate liquids containing Fe_2O_3 and the effect of composition, temperature, oxygen fugacity and pressure on their redox states. *Contrib. Mineral. Petrol.*, 108, 82–92.

Maeno, F., Suzuki, Y., Nakada, S., Koyama, E., Kaneko, T., Fujii, T., Miyamura, J., Onizawa, S., and Nagai, M. (2010). Course and ejecta of the eruption of Asama Volcano on 2 February 2009. *Bull. Volcanol. Soc. Jpn.*, 55, 147–154.

Martin, R. S., Roberts, T. J., Mather, T. A., and Pyle, D. M. (2009). The implications of H_2S and H_2 kinetic stability in high-T mixtures of magmatic and atmospheric gases for the production of oxidized trace species (e.g., BrO and NOx). *Chem. Geol.*, 263, 143–150.

Matjuschkin, V., Blundy, J. D., and Brooker, R. A. (2016). The effect of pressure on sulphur speciation in mid- to deep-crustal arc magmas and implications for the formation of porphyry copper deposits. *Contrib. Mineral. Petrol.*, 171, article no. 66.

Matsuo, S. (1962). Establishment of chemical equilibrium in the volcanic gas obtained from the lava lake of Kilauea, Hawaii. *Bull. Volcanol.*, 24, 59–71.

Menyailov, I. A., Nikitina, L. P., Shapar, V. N., and Pilipenko, V. P. (1986). Temperature increase and chemical change of fumarolic gases at Momotombo Volcano, Nicaragua, in 1982–1985: Are these indicators of a possible eruption? *J. Geophys. Res. Solid Earth*, 91, 12199–12214.

Métrich, N., Berry, A. J., O'Neill, H. St. C., and Susini, J. (2009). The oxidation state of sulfur in synthetic and natural glasses determined by X-ray absorption spectroscopy. *Geochim. Cosmochim. Acta*, 73, 2382–2399.

Moussallam, Y., Edmonds, M., Scaillet, B., Peters, N., Gennaro, E., Sides, I., and Oppenheimer, C. (2016). The impact of degassing on the oxidation state of basaltic magmas: A case study of Kīlauea volcano. *Earth Planet. Sci. Lett.*, 450, 317–325.

Moussallam, Y., Longpré, M.-A., McCammon, C., Gomez-Ulla, A., Rose-Koga, E. F., Scaillet, B., Peters, N., Gennaro, E., Paris, R., and Oppenheimer, C. (2019a). Mantle plumes are oxidised. *Earth Planet. Sci. Lett.*, 527, article no. 115798.

Moussallam, Y., Oppenheimer, C., and Scaillet, B. (2019b). On the relationship between oxidation state and temperature of volcanic gas emissions. *Earth Planet. Sci. Lett.*, 520, 260–267.

Moussallam, Y., Oppenheimer, C., Scaillet, B., Gaillard, F., Kyle, P., Peters, N., Hartley, M., Berlo, K., and Donovan, A. (2014). Tracking the changing oxidation state of Erebus magmas, from mantle to surface, driven by magma ascent and degassing. *Earth Planet. Sci. Lett.*, 393, 200–209.

Nakada, S. and Motomura, Y. (1999). Petrology of the 1991–1995 eruption at Unzen: effusion pulsation and groundmass crystallization. *J. Volcanol. Geotherm. Res.*, 89, 173–196.

Ohba, T., Hirabayashi, J., Nogami, K., Kusakabe, M., and Yoshida, M. (2008). Magma degassing process

during the eruption of Mt. Unzen, Japan in 1991 to 1995: Modeling with the chemical composition of volcanic gas. *J. Volcanol. Geotherm. Res.*, 175, 120–132. Scientific drilling at Mount Unzen.

Ohba, T., Hirabayashi, J., and Yoshida, M. (1994). Equilibrium temperature and redox state of volcanic gas at Unzen volcano, Japan. *J. Volcanol. Geotherm. Res.*, 60, 263–272.

Ohwada, M., Kazahaya, K., Mori, T., Kazahaya, R., Hirabayashi, J., Miyashita, M., Onizawa, S., and Mori, T. (2013). Sulfur dioxide emissions related to volcanic activity at Asama volcano, Japan. *Bull. Volcanol.*, 75, article no. 775.

Oppenheimer, C., Scaillet, B., Woods, A., Sutton, A. J., Elias, T., and Moussallam, Y. (2018). Influence of eruptive style on volcanic gas emission chemistry and temperature. *Nat. Geosci.*, 11, 678–681.

Putirka, K. D. (2008). Thermometers and barometers for volcanic systems. *Rev. Mineral. Geochem.*, 69, 61–120.

Rose-Koga, E. F., Bouvier, A.-S., Gaetani, G. A., Wallace, P. J., Allison, C. M., Andrys, J. A., de la Torre, C. A., Barth, A., Bodnar, R. J., Gartner, A. J. J. B., Butters, D., Castillejo, A., Chilson-Parks, B., Choudhary, B. R., Cluzel, N., Cole, M., Cottrell, E., Daly, A., Danyushevsky, L. V., DeVitre, M. J., Drignon, M. J., France, L., Gaborieau, M., Garcia, M. O., Gatti, E., Genske, F. S., Hartley, M. E., Hughes, E. C., Iveson, A. A., Johnson, E. R., Jones, M., Kagoshima, T., Katzir, Y., Kawaguchi, M., Kawamoto, T., Kelley, K. A., Koornneef, J. M., Kurz, M. D., Laubier, M., Layne, G. D., Lerner, A., Lin, K.-Y., Liu, P.-P., Lorenzo-Merino, A., Luciani, N., Magalhães, N., Marschall, H. R., Michael, P. J., Monteleone, B. D., Moore, L. R., Moussallam, Y., Muth, M., Myers, M. L., Narváez, D. F., Navon, O., Newcombe, M. E., Nichols, A. R. L., Nielsen, R. L., Pamukcu, A., Plank, T., Rasmussen, D. J., Roberge, J., Schiavi, F., Schwartz, D., Shimizu, K., Shimizu, N., Thomas, J. B., Thompson, G. T., Tucker, J. M., Ustunisik, G., Waelkens, C., Zhang, Y., and Zhou, T. (2021). Silicate melt inclusions in the new millennium: A review of recommended practices for preparation, analysis, and data presentation. *Chem. Geol.*, 570, article no. 120145.

Saito, G., Ishizuka, O., Ishizuka, Y., Hoshizumi, H., and Miyagi, I. (2018). Petrological characteristics and volatile content of magma of the 1979, 1989, and 2014 eruptions of Nakadake, Aso volcano, Japan. *Earth Planets Space*, 70, article no. 197.

Sandanbata, O., Obara, K., Maeda, T., Takagi, R., and Satake, K. (2015). Sudden changes in the amplitude-frequency distribution of long-period tremors at Aso volcano, southwest Japan. *Geophys. Res. Lett.*, 42, 10256–10262.

Schipper, C. I. and Moussallam, Y. (2017). Temporal redox variation in basaltic tephra from Surtsey volcano (Iceland). *Bull. Volcanol.*, 79, article no. 71.

Shimano, T., Iida, A., Yoshimoto, M., Yasuda, A., and Nakada, S. (2005). Petrological characteristics of the 2004 eruptive deposits of Asama volcano, central Japan. *Bull. Volcanol. Soc. Jpn.*, 50, 315–332.

Shinohara, H., Giggenbach, W. F., Kazahaya, K., and Hedenquist, J. W. (1993). Geochemistry of volcanic gases and hot springs of Satsuma-Iwojima, Japan: following Matsuo. *Geochem. J.*, 27, 271–285.

Shinohara, H., Ohminato, T., Takeo, M., Tsuji, H., and Kazahaya, R. (2015). Monitoring of volcanic gas composition at Asama volcano, Japan, during 2004–2014. *J. Volcanol. Geotherm. Res.*, 303, 199–208.

Shinohara, H., Yokoo, A., and Kazahaya, R. (2018). Variation of volcanic gas composition during the eruptive period in 2014–2015 at Nakadake crater, Aso volcano, Japan. *Earth Planets Space*, 70, article no. 151.

Sigvaldason, G. E. and Elísson, G. (1968). Collection and analysis of volcanic gases at Surtsey Iceland. *Geochim. Cosmochim. Acta*, 32, 797–805.

Symonds, R. B., Gerlach, T. M., and Reed, M. H. (2001). Magmatic gas scrubbing: implications for volcano monitoring. *J. Volcanol. Geotherm. Res.*, 108, 303–341.

Symonds, R. B., Rose, W. I., Bluth, G. J. S., and Gerlach, T. M. (1994). Volcanic-gas studies; methods, results, and applications. *Rev. Mineral. Geochem.*, 30, 1–66.

Venezky, D. Y. and Rutherford, M. J. (1999). Petrology and Fe–Ti oxide reequilibration of the 1991 Mount Unzen mixed magma. *J. Volcanol. Geotherm. Res.*, 89, 213–230.

Zelenski, M. E., Fischer, T. P., de Moor, J. M., Marty, B., Zimmermann, L., Ayalew, D., Nekrasov, A. N., and Karandashev, V. K. (2013). Trace elements in the gas emissions from the Erta Ale volcano, Afar, Ethiopia. *Chem. Geol.*, 357, 95–116.